Food Chemistry: X 18 (2023) 100635

Contents lists available at ScienceDirect

Food Chemistry: X

journal homepage: www.sciencedirect.com/journal/food-chemistry-x

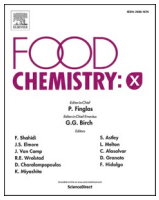

Combination with litchi procyanidins under PEF treatment alters the physicochemical and processing properties of inulin

Yuqi Huang [a], Ziqi Guo [a], Zhe Chen [a], Dan Lei [a], Shuyi Li [a,*], Zhenzhou Zhu [a,*], Francisco J. Barba [b], Shuiyuan Cheng [a]

[a] National R&D Center for Se-rich Agricultural Products Processing, Hubei Engineering Research Center for Deep Processing of Green Se-rich Agricultural Products, School of Modern Industry for Selenium Science and Engineering, Wuhan Polytechnic University, Wuhan 430023, PR China
[b] Nutrition and Food Science Area, Preventive Medicine and Public Health, Food Science, Toxicology and Forensic Medicine Department, Faculty of Pharmacy, Universitat de València, Avda. Vicent Andrés Estellés, s/n, 46100 Burjassot, València, Spain

ARTICLE INFO

Keywords:
Inulin-procyanidin complex
Pulsed electric field treatment
Characterization
Physicochemical properties

ABSTRACT

A novel alternative to prepare the inulin-procyanidin complex assisted by pulsed electric field (PEF) treatment was explored in this study. Results showed that the optimal condition of PEF treatment enhanced the adsorption rate of procyanidins to inulin from 78.56 to 103.46 μg/mg. Based on well fitted by *Redlich-Peterson* model and spectral analysis including UV and FT-IR, the interaction between inulin and procyanidin was evidenced to be dominated by hydrogen bonds. The DSC curve and the SEM spectrum displayed better stability of the PEF-treated inulin-procyanidin complex than the untreated complex. The PEF-treated complex had lower solubility but higher water-holding capacity than inulin, which exhibited stronger shear-thinning property and more stable flow behavior referring to rheological analysis. Furthermore, the gel formed from the PEF-treated complex possessed greater hardness, chewiness and viscosity, with no significant effects noted in terms of springiness, cohesiveness and resilience.

1. Introduction

Procyanidins (PCs), are a class of typical phenolic compounds, which are well known for their excellent oxidation resistance and health-promoting properties. A variety of potential bioactivities of PCs, such as anti-cancer, anti-inflammatory, anti-atherosclerosis, and cardioprotective properties as well as lipid peroxidation inhibitory effects, have been reported in previous studies (Yang et al., 2021). Rich in PCs, especially A-types (Sui, Zheng, Li, Li, Xie, & Sun, 2016), litchi pericarp is considered a promising source of dietary polyphenols, following the global trend of sustainable development. It has been demonstrated by our team that litchi pericarp oligomeric PC (LPPC), involving (−)-epicatechin, procyanidin A2, epicatechin-(4β → 8,2β → O → 7)-epicatechin, and A-type procyanidin trimer, have a strong free radical scavenging activity, regulating hepatic and muscle glucose metabolism, and attenuating atherosclerosis and hyperlipidemia in mice fed with high fat diet (X. Li, Wu, Sui, Li, Xie, & Sun, 2018). Nevertheless, as a key factor affecting beneficial effects, low bioavailability seriously restricts the commercial development and application of PCs.

Dietary fiber is proposed as the food component most probable to improve the bioaccessibility, bioavailability, and bioefficacy of PCs (Liu, Renard, Rolland-Sabaté, & Le Bourvellec, 2021). Inulin, a mixture of oligosaccharides and polysaccharides, is a soluble dietary fiber and indigestible carbohydrate, which is widely used as a low-calorie alternative to sugar and fat in the food industry because of its techno-functional attributes (Zhu, Luo, Yin, Li, & He, 2018). As a natural renewable polysaccharide resource, it can be produced from various plants in nature or even, more recently, from bio-based productions (Tripodo & Mandracchia, 2019). Since there are numerous studies of inulin connecting with beneficial effects, inulin has received extensive attention, especially when it is regarded as a prebiotic to modulate intestinal microflora and improve the intestinal environment (Zhu et al., 2019). On one hand, inulin can protect polyphenols, delaying their chemical degradation and improving their stability (Tarone, Silva, Betim Cazarin, & Marostica Junior, 2021). On the other hand, it can also help unabsorbed polyphenols to reach the colon, where they can be released by bacterial action, then be absorbed and show potential beneficial effects (Jakobek & Matić, 2019). That is to say, the

* Corresponding authors at: School of Modern Industry for Selenium Science and Engineering, Wuhan Polytechnic University, No. 68 Xue Fu South Road, 430023 Wuhan, China.
E-mail addresses: lishuyisz@sina.com (S. Li), zhenzhouzhu@126.com (Z. Zhu).

https://doi.org/10.1016/j.fochx.2023.100635
Received 16 August 2022; Received in revised form 24 February 2023; Accepted 7 March 2023
Available online 10 March 2023

combination of LPPC with inulin could be an effective approach to advance LPPC to become more available and to exert its functional properties in the human body, so it can be widely used in the food, pharmaceutical, cosmetic industries, and so forth. Intriguingly, it was further found by our lab that the complexation of inulin with polyphenols, such as epicatechin and its oligomers, enhanced the antioxidant activity and solubility of polysaccharides, with higher stability, thereby expanding their application in the food industry. However, it was reported that the absorption of polyphenols on inulin is limited, coupled with low yield of the complex (Li, Lei, et al., 2021). Hence, it is necessary to explore food-acceptable strategies to improve the absorption of polyphenols by inulin, which further promotes the development of healthier, more nutritious functional components and products.

Recent studies have shown that some innovative technologies such as high-pressure, ultrasound, and pulsed electric field (PEF) can also impact interactions between food nutrients (Li, Zhang, et al., 2021; Niu et al., 2020). Among them, PEF treatment has indicated great application potential because its non-thermal characteristic can minimize the changes in physical, chemical, and nutritional properties, while extracting, preserving, or even improving the bioavailability of more health-related food ingredients, especially phenols (López-Gámez, Elez-Martínez, Martín-Belloso, & Soliva-Fortuny, 2021). Historically, PEF has been widely applied in food processing such as the inactivation of microorganisms, extraction of active ingredients, and modification of biomolecules, which may involve electroporation, biofilm permeabilization, etc (Niu et al., 2020). A study has found that PEF could not only induce ionization of the functional groups in the macromolecules, but also break electrostatic interactions in macromolecular chains, leading to cleavage or coalescence of monomeric units (Giteru, Oey, & Ali, 2018). Moreover, the enhanced mass transfer associated with PEF can increase the chance of collisions between reacting molecules or ions (Zhang, Han, Zeng, & Wang, 2017), as well as the macromolecular interactions by changing the structure, polarizing the compounds and exposing adsorption sites (Jin et al., 2020). We have previously evidenced that PEF could facilitate the combination of LPPC and inulin, indicating the potential of better sensory quality (Manjón, Li, Dueñas, García-Estévez, & Escribano-Bailón, 2023), better antioxidant activity (Zhang, Zhang, Chen, Ma, & Xia, 2021), gut microbiota regulation ability and more stable antibacterial activity (Wang, Xie, & Sun, 2021) of the complex. However, the mechanism of interaction and the physicochemical properties and processing properties of the complex are still unclear.

In this study, we aimed to investigate the effect of PEF on the interaction between inulin and LPPC and the mechanism. In addition, the physicochemical and processing properties of the complex were also identified in order to further evaluate the alteration in polysaccharide properties.

2. Materials and methods

2.1. Chemicals and materials

Dried Fibruline® XL (FXL, average DP $\geq$ 23, purity of inulin>94.5%) was bought from Cosucra (Belgium). Fruit of litchi (Litchi chinensis Feizixiao) were obtained from Wushang Supermarket, which were peeled as soon as possible when arrived at laboratory. The pericarp was stored at −18°C until used. LPPC was prepared according to Li's method (S. Li et al., 2012). Frozen lychee peel fragments were extracted using 70% ethanol at 50 °C for 1.5 h. The fraction eluted by 70% ethanol was collected after separation on an AB-8 resin (weak polarity macroporous resin, 0.3–1.25 mm particle size, Nankai Hecheng Science & Technology Co., Tianjin, China) column (hotmelt glass, 15 × 3.5 cm, ID, Labmart Scientific Instruments Co. Ltd., Beijing, China). The eluate was evaporated and then extracted by ethyl acetate to obtain LPPC. All other chemicals were of analytical grade.

2.2. Preparation of LPPC complex and the physical mixture

Primarily, inulin (200 mg) was dissolved in 100 mL of pure water at 80 °C with magnetic stirring. Then the solution was put aside until it reached room temperature. Meanwhile, LPPC (50 mg) was poured into 50 mL of pure water and stirred to be completely dissolved, and the two pretreated solutions were mixed up. After blending, the conductivity value of the mixed solution at room temperature measured by the conductivity meter (Mettler-Toledo SevenCompact™ conductivity meters S230, Shanghai, China) was 1523μS/cm. PEF treatment (THU-PEF4, Xintianpu, China) was applied to the system. The mixed solution flows in from below, through a spherical treatment chamber with a diameter of 3 mm, and out from above it. Prior to operation, the bubbles in the system should be eliminated by pumping part of the mixed solution. With fixed exponential pulse width of 50 μs and frequency of 1.02 kHz, the influence of the electric field intensity (6.7–26.7 kV/cm) and the PEF treatment time (1.62×10^{-3}-2.59×10^{-3} s obtained by variation of flow rate (2–1.25 mL/s) and 8.63×10^{-4}-7.77×10^{-3} s obtained by variation of sample cycles (1–9)) on adsorption capacity (Q_e) were explored.

The solution treated by PEF was transferred into a dialysis bag (MD45, 1kDa, Solaibio). Then it was dialyzed against 3000 mL of water for about 48 h to achieve equilibrium when the continuous value of absorbance outside the dialysis bag was changeless at 280 nm. The solution inside the dialysis bag was concentrated, precipitated by alcohol and freeze dried. The dried light-pink powder was collected as the complex of LPPC and inulin. Besides, the inulin complex formed without PEF treatment was also prepared that went through the same process.

The quality of LPPC outside the dialysis bag was calculated with the help of the working curve of UV absorbance (A)-LPPC concentration (C). The absorbance value of a series of LPPC solutions (0.005–0.040 mg/mL) was measured, the fitted regression equation being $A = 9.9151C + 0.0131$ ($R^2 = 0.9998$). The content of LPPC in the complex was approximate 10%. According to the amount of procyanidin absorbed in the inulin complex, the physical mixture of these two components was prepared with the same mass ratio.

2.3. Equilibrium dialysis assays

The adsorption capacity (Q_e) during dialysis equilibrium, in terms of the quality(μg) of LPPC absorbed by 1 mg of inulin, can be represented by the following equation (Gao, Liu, Peng, Wu, Wang, & Zhao, 2012).

$$Adsorption \quad capacity(Q_e, \mu g \quad mg^{-1}) = \frac{M_{LPPC} - C_e V}{M_{inulin}} \tag{1}$$

where M_{LPPC} is the mass of LPPC (μg), C_e is the concentration of LPPC outside the dialysis bag (μg·mL^{-1}), V is the total volume of solution in the dialysis system (mL), and M_{inulin} is the mass of inulin (mg).

2.4. Adsorption isotherm models

In order to explore the characteristics and mechanism of the adsorption process, the experimental results of Q_e on C_e were applied to the *Langmuir*, *Redlich-Peterson* and *Toth* adsorption isotherms. Table S1 summarizes the isothermal model equations adopted in this study. Besides, the coefficient of determination (r^2) was used to evaluate the effectiveness of the model.

2.5. Spectrographic and physicochemical properties of different complexes

2.5.1. Ultraviolet spectroscopy

Different samples were dissolved respectively, including inulin, LPPC, untreated complex, the PEF-treated complex and the physical mixture of inulin and LPPC. The UV spectroscopies of the above-mentioned solutions were recorded respectively using an UV-220

spectrophotometer (Thermo Scientific, America) in the wavelength ranging from 200 and 400 nm.

2.5.2. Fourier transform infrared spectroscopy (FT-IR)

FT-IR spectra of samples were obtained using a NEXUS 670 FT-IR spectrophotometer (Nicolet, USA) in the range 4000–400 cm^{-1} by the KBr method (Li, Lei, et al., 2021).

2.5.3. Differential scanning calorimetry (DSC)

The DSC curves were measured by a DSC instrument (Q2000, TA, USA). About 2 mg of dried, pulverous samples were respectively settled in aluminum sample boxes. An empty aluminum sample box was used for reference. The boxes were programmed at a heating rate of 10 °C/min from 50 to 270 °C.

2.5.4. Scanning electron microscopy (SEM)

The dried samples were dropped apart on the clean surface of aluminum-foil paper. After being treated by spray-gold, all the samples were evaluated under the SEM (S-3000 N, Hitachi, Japan) (Li, Lei, et al., 2021).

2.6. Processing characteristics of the PEF-treated complex

2.6.1. Water solubility and water holding capacity

The solubility and water holding capacity of inulin and the PEF-treated complex were determined according to the method reported by (Luft et al., 2021). Appropriate amounts (m_1) of inulin or complex were added to 2 mL centrifuge tubes containing 1 mL of distilled water. These centrifuge tubes were placed in a constant temperature water bath at 20, 30, 40, 50, 60, and 70 °C respectively for 2 h, and then left to stand for 8 h, during which process it was ensured that the inulin or the complex could not be completely dissolved. Then the suspensions were centrifuged at 5000 rpm for 40 min, and after removing the supernatant, the precipitates were dried at 50 °C to a constant weight to obtain the dry solid weight (m_2). The water solubility was calculated according to the following formula:

$$Solubility\ (\%) = \frac{m_1 - m_2}{m_1} \times 100 \quad (2)$$

where m_1 is the mass (g) of the solute added and m_2 is the dry weight (g) of precipitant.

A certain amount of inulin or complex powder and 1 mL of distilled water was added into 2 mL centrifuge tubes. After mixing thoroughly in a water bath at 20, 30, 40, 50, 60, and 70 °C, they were left in the water bath for 8 h. The suspensions were centrifuged at 5000 rpm for 60 min, and after removing the supernatant, the mass of precipitates was recorded as m_3. The precipitate was dried at 50 °C to a constant weight and the mass was recorded as m_2. The water holding capacity was calculated according to the following formula:

$$Water\ holding\ capacity\ (\%) = \frac{m_3}{m_2} \times 100 \quad (3)$$

where m_3 is the wet weight (g) of the precipitate and m_2 is the dry weight (g) of precipitant.

2.6.2. Steady flow behavior

The rheological behaviors of inulin and the PEF-treated complex were measured with a HR-2 Hybrid Rheometer (TA Instruments, New Castle, Delaware, USA), using a cone plate (40 mm in diameter, angle 2°, gap of 1 mm). Changes in the apparent viscosities (τ) of inulin and complex at concentrations of 1–100 mg/mL in the shear rate (γ) range of 10 to 100 s^{-1} were detected through the method by (Ding, Liu, Ye, Zhang, & Wang, 2021) with slight modification. The power-law model was applied to describe the structural state of the system:

$$\tau = k_c \gamma^{n-1} \quad (4)$$

where k_c is the consistency index (mPa·s) and n is the flow behavior index.

2.6.3. Textural properties

40% of inulin and the PEF-treated complex solutions were prepared respectively, and then they were placed in a water bath at 90 °C for heating. After cooling, they were transferred to 4 °C for refrigeration treatment until the gels formed. After aging at room temperature for 30 min, texture profile analysis was performed on the inulin and the complex gel using a TA.XTplus Texture Analyzer (Stable Micro Systems, London). The gel puncture depth was 10 mm, the probe diameter was 0.5 cm, the puncture rate was 1 mm/s, and the trigger force was 5 g. The data were analyzed by the software Bluehill that came with the instrument, and each group of experiments was repeated for three times.

2.7. Statistical analysis

All experiments were repeated for three times and the results were displayed as the mean ± standard deviation (SD) of the repetitions. Duncan's multiple range tests was performed to evaluate significance by using SPSS software (version 19.0, SPSS Inc., Chicago, IL, USA) ($p < 0.05$). The plotting of the functional relationship between adsorption capacity Q_e and equilibrium concentration C_e, as well as the nonlinear model fitting of the different models was performed by using an Origin Software (Systat Software Inc., Version 8.0).

3. Results and discussion

3.1. Effect of PEF on the adsorption of LPPC to inulin

As a key factor, the effect of electric field intensity on adsorption capacity was explored and the results were shown in Fig. 1A. With the increase of electric field intensity, the adsorption capacity increased first and then decreased, reaching the maximum (103.46 ± 0.27 μg/mg) when the electric field intensity was 13.3 kV/cm. Compared with the untreated complex, the adsorption capacity of the PEF-treated complexes was significantly improved in Fig. 1A. With the help of PEF treatment, part of the energy could be absorbed by the molecular chain of inulin, which had potential to alter the configuration of inulin and expose hydrophobic groups, increasing the adsorption sites to polyphenols. Previous studies convinced that PEF treatment could change the configuration of the molecular chain through particle orientation effects and perturbations (Liu, Zhang, Zeng, El-Mashad, Pan, & Wang, 2014). However, under high electric field intensity (E > 13.3 kV/cm), it displayed a downward trend in the adsorption capacity. There are two possible reasons for this phenomenon. Firstly, as the electric field intensity strengthened, deeper changes in the structure of inulin appeared, which may involve disruption of electrostatic interactions in the macromolecular chain, leading to cleavage or agglomeration of monomer units (Giteru et al., 2018). Further, it affected the interaction with LPPC, inducing a decrease in the adsorption capacity. This view was in agreement with a previous study by Liu et al (Liu, Lopez Sanchez, Martinez Sanz, Gilbert, & Gidley, 2019), who reported that modification of composition and organization of polysaccharides could influence their interaction with polyphenols, especially affecting the structural features of the polysaccharide. Secondly, high electric field intensity may also break the bond of the newly formed complex, giving rise to a decrease in the adsorption of LPPC to inulin. A similar trend was also found in PEF-assisted BSA/starch conjugates. The decrease in the grafting degree may be a result of the degradation of the conjugates at high electric field strengths (Taha et al., 2022). Therefore, the electric field was chosen as 13.3 kV/cm in the following steps.

As shown in Fig. 1B, the slower the flow rate is, the higher the adsorption capacity can be. During the processing, the sample was sucked into the reactor chamber by the pump. When the flow rate was

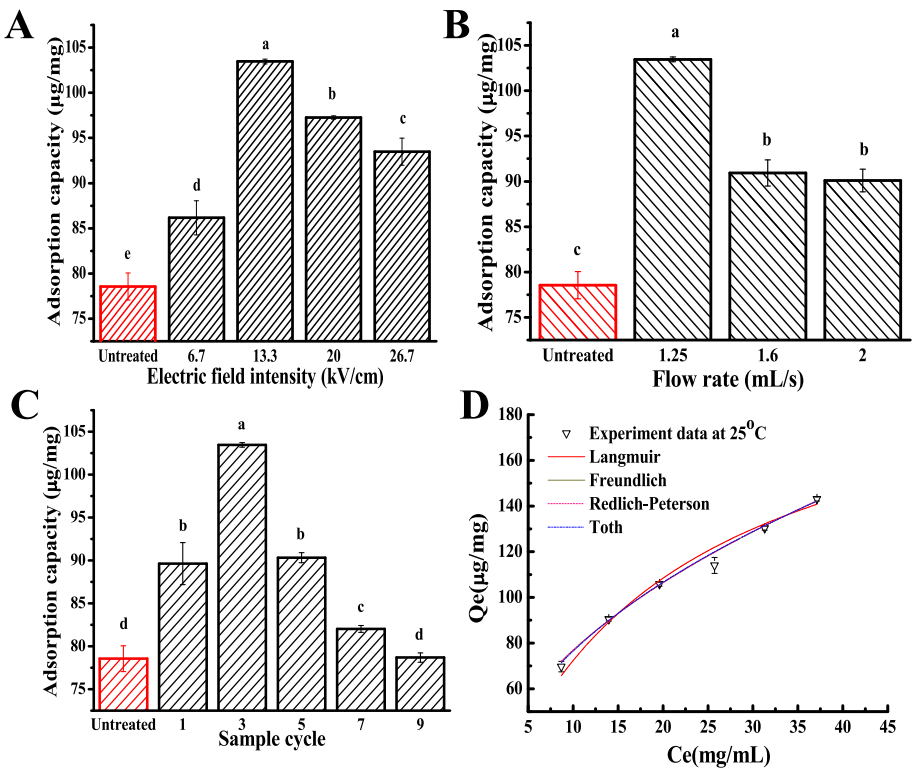

Fig. 1. Effects of electric field intensity (A), flow rate (B), and sample cycle (C) on the adsorption capacity of LPPC to inulin. Values are given as the means of three independent experiments, and error bars represent the SD. Different lower-case letters indicate significant difference ($p < 0.05$). (D) Adsorption modeling experiment performed at room temperature 25 °C, 200 mL of 2 mg/mL inulin, 50 mL of LPPC aqueous solution with known concentrations, and PEF treatment with optimal parameters.

slow, the residence time of the sample in the chamber would be longer, improving the energy input to promote the adsorption. If the flow rate is too slow, the sample cannot be easily sucked into the chamber. To further explore the effect of extending treatment time on the adsorption capacity, different sample cycle ranging from 1 to 9 was studied.

It can be seen that a similar trend as the effect of electric field intensity was depicted in Fig. 1C. When the treating time prolonged by increasing the sample cycle from 1 to 3, the adsorption capacity elevated from 89.63 ± 2.45 to 103.46 ± 0.27 μg/mg. Besides, with further enrichment of the sample cycle, a significant reduction of the adsorption capacity was observed. The reason for this phenomenon may be due to the variation of pH after the excessive processing time, which was also detected by Zhang et al. They found that the long time PEF treatment could alter the pH value of the solution, arousing the prevention of the interaction and the acceleration of the dissociation processing of the complex (Zhang et al., 2017). Moreover, some previous studies have revealed that pH has a great impact on the interactions between polyphenols and macromolecular materials, including polysaccharides (Gao et al., 2012). This impact can be explained by the amount of protonated and deprotonated functional groups, or the ratio of protonated/deprotonated molecules, which can exert influence on the various attractive or repulsive forces between interacting molecules (Jakobek & Matić, 2019). On the whole, the optimized operating condition of PEF treatment was described as follows: the electric field intensity was 13.3 kV/cm, flow rate was 1.25 mL/min, and sample cycle was 3. Under this condition, the maximum adsorption capacity was 103.46 ± 0.27 μg/mg, an increase of 31.71% compared to the untreated complex.

3.2. Adsorption model analysis

The adsorption process is a surface phenomenon in which adsorbate molecules (procyanidin) interact physically or chemically with the surface of the adsorbent molecules (inulin). Adsorption isotherm can describe the qualitative information of the interaction between the adsorbent and the adsorbate and the quantitative relationship between the equilibrium adsorption capacity (Q_e) of the absorbent and the equilibrium concentration (C_e) of the adsorbate at a constant temperature (Gao et al., 2012). With PEF pre-treatment at optimal condition (field intensity was 13.3 kV/cm, flow rate was 1.25 mL/min, and sample cycle was 3), 200 mL of 2 mg/mL inulin and 50 mL of LPPC aqueous solution with known concentrations (0.8, 1.2, 1.6, 2.0, 2.4, and 2.8 mg/mL) were chosen for the adsorption experiment at 25 °C. The amounts of LPPC absorbed to inulin were increased approximately linearly with the concentration of LPPC from 0.8 to 2.8 mg/mL (Fig. 1D). This suggested that there was equilibrium between free and bound LPPC, whereas the increase of concentration would lead to an increase in binding capacity.

In order to establish the possible maximum binding capacities and deduce the adsorption mechanism of procyanidins to inulin, the experiment data are depicted by *Langmuir*, *Freundlich*, *Redlich-Peterson* and *Toth* empirical binding isotherm models through non-regression analysis method (Fig. 1D). The fitted model equations and determination coefficient (R^2) are summarized in Table 1. It can be seen from the result that the experimental data were well-fitted by all of the four isotherm formulas ($R^2 > 0.98$). However, *Freundlich*, *Redlich-Peterson*, and *Toth* models fitted better than *Langmuir* isotherm model. Besides, the value of R^2 for *Redlich-Peterson* isotherm model is the highest, indicating that the equilibrium data for the adsorption of procyanidins to inulin might be adequately characterized in terms of the *Redlich-Peterson* isotherm model. As mentioned in previous studies, *Redlich-Peterson* isotherm model is a combination of the *Langmuir* and *Freundlich* isotherm model,

Table 1
Isotherm parameters and equations obtained using the nonlinear method for the adsorption of LPPC to inulin.

Isotherm type	Equation	R^2
Langmuir	$Q_e = \frac{216.09495 \times 0.05034C_e}{1 + 0.05034C_e}$	0.98798
Freundlich	$Q_e = 26.12413C_e^{0.46891}$	0.99584
Redlich-Peterson	$Q_e = \frac{1504.79649C_e}{1 + 57.08511C_e^{0.53289}}$	0.99688
Toth	$Q_e = \frac{100977.57177C_e}{\left(1/0.84797 + C_e^{0.09307}\right)^{1/0.09307}}$	0.99565

which improves the limitation of *Langmuir* isotherm model by high concentration conditions and *Freundlich* isotherm model by low concentration conditions (Gao et al., 2012). When the exponent β is 1, it can be considered as *Langmuir* isotherm model. Conversely, when the exponent β is not 1, and the constant 'a' is much bigger than 1, it can be regarded as *Freundlich* isotherm model, which is absolutely the condition of the fitted model equation of *Redlich-Peterson* isotherm model. Therefore, the adsorption process related to multilayer coverage, as well as various adsorption properties existed in the interaction between LPPC and inulin. Previous studies also reported the adsorption of luteolin to CSP2 using this approach, indicating the heterogeneous surface of CSP2, and their adsorption is not restricted to a monolayer approach (Guo, Ma, Xue, Gao, & Chen, 2018). Furthermore, *Redlich-Peterson* isotherm model not only had the adsorption characteristics of the *Freundlich* isotherm model but the adsorption process would not be limited by the low concentration.

3.3. Physicochemical Characterization of the PEF-treated complex

3.3.1. UV absorption spectrum

UV spectroscopy has been widely applied to characterize the interaction between polyphenols and macromolecules (Lei et al., 2022). In Li's study, the soluble dietary fiber in lotus root successfully adsorbed gallic acid (GA) and catechin (CC), respectively, which was determined via UV and FT-IR spectra (S. Li, Li, Zhu, Cheng, He, & Lamikanra, 2020). The kind of flavonoid grafted with polysaccharides, grafting methods, and grafting efficiency can also be determined by the position and quantitative relationship of the characteristic UV absorption peaks (S. Li et al., 2020). The obtained absorption spectra of inulin, LPPC, their physical mixture, the untreated complex, and the PEF-treated complex were presented in Fig. 2A. In the spectrum of LPPC, a λ_{max} value was found at 280 nm due to the abundant flavan-3-ols (π-π* transition of the phenolic group) in the extract (Wu et al., 2011), which did not appear in the spectrum of inulin. Thus, the change of absorption peak at 280 nm can indicate the change in the structure and content of procyanidins. The spectrum of the physical mixture was identical to that of LPPC, but the absorption peak of the untreated complex and the PEF-treated complex totally disappeared, which implied that the procyanidins in the inulin-procyanidin complex solution weren't in free form anymore. It may be the result of the interaction between polyphenol and polysaccharide, related to the combination of hydrogen bonding and hydrophobic interaction, which is similar to the interaction between phenolic compounds and lotus root polysaccharides (LRPs) (Yi, Tang, Sun, Xu, Min, & Wang, 2022).

3.3.2. FT-IR analysis

FT-IR is commonly used to characterize structural changes in the interaction of large and small molecules. The formation of complexes of seven anthocyanin components from GSAE with Gli was determined based on UV and FT-IR analysis(Z. Guo et al., 2022). The FT-IR spectrums of LPPC, inulin, their physical mixture, untreated complex, and the PEF-treated complex were depicted to verify the successful formation of procyanidin and inulin complex (Fig. 2B). For LPPC, the wide peak around 3400 cm^{-1} was related to –OH stretching vibration and the characteristic absorption peak at 1610 cm^{-1}, 1518 cm^{-1}, 1415 cm^{-1}, 1283 cm^{-1} was assigned to the aromatic nucleus (Jing, Huang, & Yu, 2019). Inulin is characterized by bands at 3410 cm^{-1}, 2928 cm^{-1}, and 1032 cm^{-1} that are assigned to OH stretching, CH_2 stretching and C—O—C bending respectively (Li, Lei, et al., 2021). For the untreated complex and the PEF-treated complex, aromatic nucleus absorption peaks largely disappeared in the FT-IR spectrum, which may overlap with the broadband peaks in 1600–1450 cm^{-1} region (Wu et al., 2011). It demonstrated that the hydroxyl groups of procyanidin interacted with the oxygen atom of inulin. It has been shown that phenolic acids could form ester linkages with structural carbohydrates and proteins through their carboxyl groups or ether linkages with lignin through the hydroxyl groups in their aromatic rings, respectively, forming bound phenolics that provide a physical and chemical barrier for cellular tissues (S. Li et al., 2022). Comparing inulin, the untreated and the PEF-treated complex, the bands detected in the wavenumber range of 2928 cm^{-1} and 1200–800 cm^{-1} existed in all of their spectrums, which were related to the stretching vibration of C—H of CH_2/CH_3 groups and represented the sugar structure of inulin, respectively. However, the C_6-OH group of inulin characterized by the band at 985 cm^{-1} disappeared and weakened in the spectrums of complexes, suggesting that procyanidin was absorbed through this part of inulin (Jing et al., 2019). Therefore, it was indicated that there are interactions between LPPC and inulin. Additionally, the FT-IR spectrum of the physical mixture of LPPC and inulin

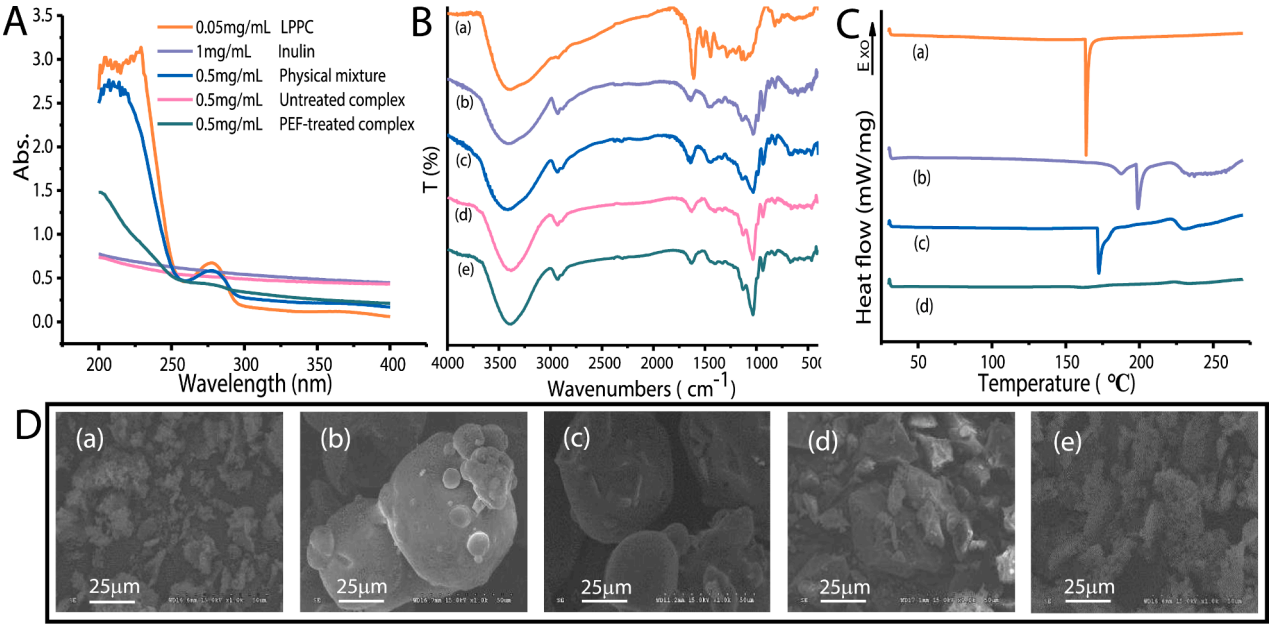

Fig. 2. (A)UV spectrum, (B)FT-IR spectrometry, and (D) SEM images of LPPC (a), inulin (b), the physical mixture (c), the untreated complex (d), and the PEF-treated complex (e). (C)DSC curves of LPPC (a), inulin (b), the physical mixture (c), and the PEF-treated complex (d).

was not significantly different from those of single components.

3.3.3. DSC analysis

According to DSC analysis of LPPC, inulin, their physical mixture, and the PEF-treated complex, their endothermic transitions were observed (Fig. 2C). The endothermic peak was located approximately at 160 °C due to the melting endotherm of LPPC (Spizzirri, Altimari, Puoci, Parisi, Iemma, & Picci, 2011). For inulin, The DSC curve showed three different endothermic transitions, the first of which was at 185 °C for the melting point of inulin (Ganie, Ali, Mir, & Mazumdar, 2019). The second peak at 200 °C corresponded to the degradation of inulin chains (Spizzirri et al., 2011). And the third peak at 230 °C was related to further degradation. However, the DSC curve of the physical mixture of LPPC and inulin showed endothermic transitions occurring at 175 °C and 230 °C due to melting and degradation. The melting of the physical mixture appeared between LPPC and inulin as well as the degradation temperature of the physical mixture is the same as that of inulin, indicating that there was no reaction between the two single components in the physical mixture. With respect to the PEF-treated complex, those peaks disappeared in the DSC of the complex, which suggested a strong interaction between LPPC and inulin (Ganie et al., 2019). Moreover, the structure thermostability of the PEF-treated complex was enhanced. This is consistent with the results obtained from a previous study (Wu et al., 2011).

3.3.4. SEM analysis

To examine the general morphology of LPPC, inulin, untreated complex, and the PEF-treated complex, and then to explain their behavior and some of their physicochemical properties, SEM was used. As shown in Fig. 2D, inulin exhibited larger spherical particles with the size ranged from 10 to 70 μm, while LPPC presented as irregularly shaped fragments. The morphology of the physical mixture of LPPC and inulin was similar to that of inulin because of the weight ratio. Notably, there was a drastic change in the morphology and shape of the inulin-procyanidin complex compared to the original extract. The untreated complex showed an irregular polyhedron with a rough surface, indicating that inter- and intra-molecular hydrogen bonds of the original inulin had been greatly reduced after binding with LPPC (Liu, Lu, Kan, Wen, & Jin, 2014). Guo et al. found the morphology of CSP changed from a smooth and close surface into a polysaccharide surface with aggregates of some particles of flavonoids after the absorption of CSF (Guo et al., 2018). A similar phenomenon was also observed in the inulin-TPP complex, appearing in the form of small and elongated shreds with alternating smooth and punctured surfaces (Li, Lei, et al., 2021).

On the other side, the microstructure of the PEF-treated complex was a flaky nature with relatively porous and large surface, which showed clear interaction between inulin and LPPC. Moreover, compared with the untreated complex, the PEF-treated complex has a more compact and oriented structure, which may be due to the PEF treatment that changes the granular structure of the macromolecules, exposing more binding sites, with higher intermolecular hydrogen bonding and hydrophobic interactions during the combination, some aggregates formed. It has been evidenced by Giteru et al. (2021) that biomacromolecules can interact with each other through complex coacervation under PEF intensities of *QP* 150–400 kJ/kg and *EP* 1.6–3.4 kV/cm, displaying the morphology of layers of loosely connected sheets in chitosan/zein/polyvinyl alcohol/polyethylene glycol composite dispersions the PEF-treated at 0.8 kV/cm (Giteru, Ali, & Oey, 2021). A similar complicated structure with lace-like morphology was detected in the ultrasound-treated inulin-TPP complex (Li, Lei, et al., 2021). The result suggested that the PEF-treated complex is optimal for promoting physical interaction.

3.4. Processing characteristics

3.4.1. Water solubility and water holding capacity

The water solubility of inulin and the PEF-treated complex at different temperatures were shown in Fig. 3A(a). As the temperature rose from 20 to 70 °C, the water solubility of both inulin and complex exhibited a gradual upward trend, and the water solubility of inulin is higher than that of the complex. Over this temperature range, the solubility of inulin was elevated from 4.81 ± 0.32% to 8.96 ± 0.22%, and the solubility of the complex increased from 2.30 ± 0.14% to 6.74 ± 0.14%, showing a higher growth rate in the solubility than inulin. Some researchers have evidenced that the water solubility of inulin is related to temperature, concentration, and degree of polymerization (Jakobek & Matić, 2019). Due to the big molecular weight (Mw) of the long-chain inulin, the aggregation of the PEF-treated complex can be higher, which can lead to a negative effect on the entrapment of polyphenols and their solubility (Jakobek & Matić, 2019). Besides, compared with inulin, the variation in water solubility of the PEF-treated complex may be related to the hydrophobic interactions and polar groups such as hydrophilic hydroxyl groups. As mentioned in the FT-IR analysis, the oxygen atom in the inulin forms a hydrogen bond with the hydroxyl group in the procyanidin. Meanwhile, mediated by hydrophobic interactions, the hydrophobic layers or the hydrophobic pockets in which polysaccharides encapsulate polyphenols can be formed (Liu, Le Bourvellec, & Renard, 2020). In this way, with the reduction of hydrophilic groups and binding sites exposed after the interaction between the two substances, the original solubility of polyphenols and polysaccharides is altered. Thus, the lower solubility can make the complex a potential alternative to long-chain inulin as a fat substitute and texture modifier.

It can be seen from Fig. 3A(b) that the water retention of inulin and the PEF-treated complex is greatly affected by temperature. With increasing temperature, the water retention of inulin and complex drops first and then grows, displaying a higher value of the complex. The water retention of inulin reaches the highest 347.47 ± 8.29% at 70 °C, while that of the complex is 401.73 ± 6.01%. Commonly, a strong water holding capacity indicates high hydrophilicity and stronger interaction with water molecules. According to the results of solubility, inulin should have a higher water-holding capacity, but the result is the opposite. This may be referring to the formation of three-dimensional helical structures between long-chain inulin molecules that may also affect the interactions with water molecules, resulting in relatively low water-holding capacity (Mensink, Frijlink, van der Voort Maarschalk, & Hinrichs, 2015). Furthermore, the PEF-treated complex has a larger specific surface (rough surface) capable of adsorbing more water than that of inulin (smooth surface). The strong water retention of the complex can perform an excellent application value in food processing such as dough products and meat products.

3.4.2. Steady shear viscosity

In order to explore the processing potential of the inulin-procyanidin complex, the rheological properties were consequently evaluated. Respectively, the dependent relationship between apparent viscosity and different concentrations of inulin and complex at a shear rate from 10 to 100 s^{-1} was detected. As illustrated in Fig. 3B, the apparent viscosity of both inulin and complex solution grew in number with the increase of concentration. Similar phenomena was also found in water-soluble polysaccharides from *Rosa roxburghii Tratt* fruit (Wang, Zhang, Xiao, Huang, Li, & Fu, 2018), which may be related to the limited movement and stretched polymer chain, because of the increase in the entanglement of molecular chains in high concentration solutions. Also, a certain ratio of polysaccharides can also increase the viscosity of the complexes and the formation of a structured gel network (Peng et al., 2022). Compared with inulin, the apparent viscosity of the complex solution (inulin-procyanidin) is higher. This may be owing to the interaction between procyanidin and inulin, leading to the increase in the flow resistance of the system caused by the relative movement of

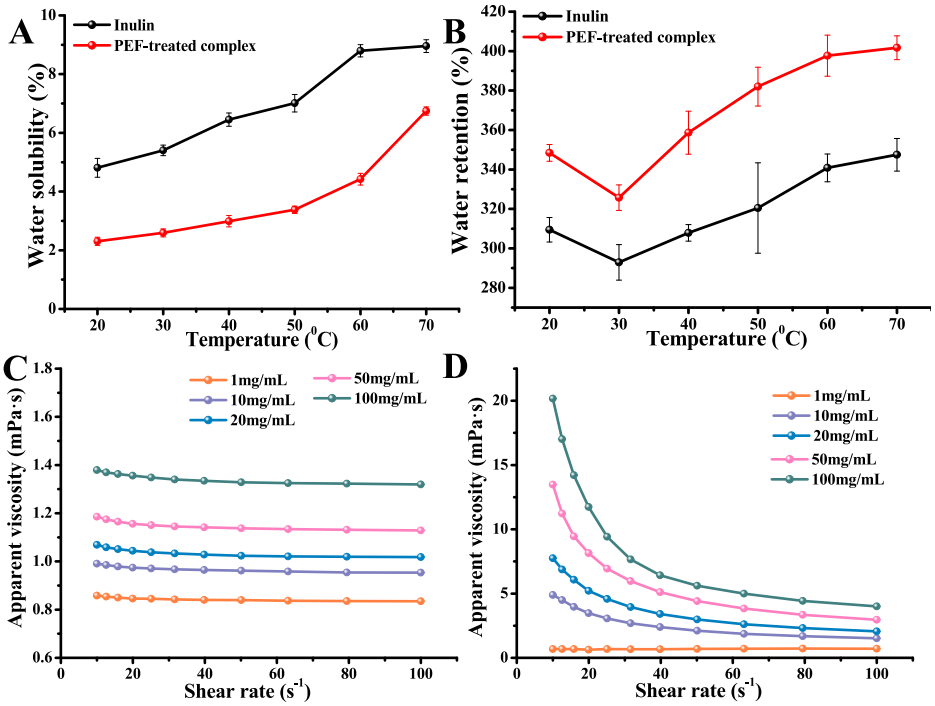

Fig. 3. (A)Water solubility (a) and water retention (b) of inulin and the PEF-treated complex. (B)The flow behavior of inulin (a) and the PEF-treated (b) at shear rates from 10 to 100 s^{-1}.

molecules. As a result, the difficulty of shearing the system increased, as the viscosity of the system. The increase in apparent viscosity of the complexes can be further attributed to the hydrogen bonding that occurs in the nearby biopolymer molecules during the formation of the complex, inducing a more entangled network (Ding et al., 2021). Currently, the characteristic of long chain inulin to improve the viscosity of the solution at lower concentration and temperature conditions has made it widely used as a thickener in the food industry. The higher apparent viscosity allows the complex to achieve the same degree of thickening at a lower concentration or a lower dosage.

Almost all inulin and complex solutions show a downward trend with the increase of shear rate, implying non-Newtonian and shear-thinning flow behaviors. Generally, the shear-thinning of polysaccharide solutions may result from the reduction of chain entanglement and the orientation effect of molecular chains under high shear rates (Lin et al., 2018). Simultaneously, it can be observed that the shear-thinning sensitivity of the complex is greater than that of inulin. As the shear rate improved, the apparent viscosity of the complex decreased largely, which corresponded to the power-law model fitting of these two kinds of solutions (Table 2). Except for the 1 mg/mL complex solution, all solutions showed non-Newtonian and pseudoplastic flow behavior ($n < 1$). This exception may be due to the fact that at low concentrations, individual molecular chains are far apart and can move freely in the solution. Hence, it is less affected by the shear force, which has almost negligible impact on the flow behavior (Shao, Qin, Han, & Sun, 2014). The complex with procyanidin reduced the value of n, the greater the concentration, the higher the pseudoplasticity (the smaller the n). In summary, the inulin-procyanidin complex prepared with PEF treatment is a typical non-Newtonian fluid. Because of its advantageous apparent viscosity and pseudoplasticity, it has a great potential for application as a functional food additive in the food industry, even in pharmaceutical, cosmetics, and other industries.

Table 2
The behavior index (n) and the consistency (k) of inulin and complex at different concentrations by Power-law model at 25 °C, R^2: coefficient index.

	Sample concentration (mg/mL)	Consistency index, k_c (mPa·s)	Flow behavior index, n	R^2
Inulin	1	0.869	0.991	0.999
	10	1.017	0.986	0.999
	20	1.087	0.985	0.999
	50	1.208	0.985	0.999
	100	1.415	0.984	0.999
PEF-treated complex	1	0.595	1.038	0.999
	10	16.234	0.482	0.998
	20	29.745	0.417	0.997
	50	56.11	0.356	0.993
	100	92.718	0.301	0.910

3.4.3. *Textural properties*

TPA is a simple and fast analysis technique that is widely used in the food industry for texture detection by compressing samples twice to imitate human chewing movements (Pan et al., 2021). As shown in Table 3, the hardness, gumminess, and chewiness of the complex were significantly higher than those of inulin, displaying an increase of 348%, 245%, and 224%, respectively ($p < 0.05$). These results may be related to the interaction between procyanidin and inulin, forming hydrogen bonds to strengthen the network structure of inulin gel. Cognate results appeared in the study of Pan et al. (2021), in which procyanidin from Chinese bayberry leaves (BLPs) was incorporated into emulsion-based oleogel to improve the gel strength by forming colloidal complexes with gelatin (Pan et al., 2021). Similarly, Staroszczyk et al. (2020) reported that the gelatin gel in fruit juice exhibited better gel strength due to the interaction between anthocyanins and gelatin (Staroszczyk, Kusznierewicz, Malinowska-Pańczyk, Sinkiewicz, Gottfried, & Kołodziejska, 2020). Moreover, it was found that proper PEF treatment can significantly improve the gelation properties of myofibrillar proteins (MPs) depending on conditions (Dong, Tian, Xu, Han, & Xu, 2021). With the assistance of PEF treatment, the dense and oriented microstructure of the complex may also contribute to the gel network. That is to say, PEF treatment promoted the formation of inulin molecules with a better capacity for re-association. Then, better formation of the network

Table 3
TPA parameters of inulin and the PEF-treated complex gels. Means with different letters (a-b) differ significantly ($p < 0.05$) among the data in the same column.

	Hardness(g)	Gumminess(g)	Chewiness(g)	Springiness	Cohesiveness	Resilience
Inulin	20.813 ± 2.121^{a}	8.183 ± 0.686^{a}	7.908 ± 1.093^{a}	0.918 ± 0.085^{a}	0.421 ± 0.056^{a}	0.009 ± 0.001^{a}
PEF-treated complex	93.247 ± 4.970^{b}	28.251 ± 1.953^{b}	25.615 ± 1.716^{b}	0.939 ± 0.054^{a}	0.307 ± 0.082^{a}	0.015 ± 0.002^{a}

Note: Values in the same column with different letters differ significantly according to the Duncan test ($p < 0.05$).

increases the hardness, chewing and gumminess of the sample. A study involving PEF enhance starch 3D printing application have demonstrated that wheat starches with specific PEF treatment showed some damage and fracture on the granule surface, and their hydrogels showed significantly ($p < 0.05$) higher firmness than those obtained from native starch(Maniglia, Pataro, Ferrari, Augusto, Le-Bail, & Le-Bail, 2021). The values of springiness, cohesiveness and resilience are respectively close, implying that the addition of procyanidin has no effect on them.

4. Conclusion

In this work, alterations in the physicochemical and processing properties of inulin by combination with litchi procyanidins under PEF treatment were investigated. The inulin-procyanidin with the highest adsorption of LPPC (103.46 μg/mg) was obtained after treated by PEF at electric field intensity of 13.3 kV/cm, flow rate of 1.25 mL/min, and sample cycles of 3. The isotherm study was successfully applied for modeling analysis of the adsorption capacity of LPPC to inulin. The fitting results showed that the adsorption of inulin to LPPC has the characteristics of multi-layer adsorption and is not limited by low concentration. The formation of the inulin-procyanidin complex was determined based on UV–Vis and FT-IR analysis, which may be related to hydrogen bonding and hydrophobic interactions. And the polysaccharide skeleton of inulin was not altered in the formed complex. Besides, the results from DSC and SEM demonstrated that the PEF-treated complex not only have good thermal stability, but also have a dense and oriented physical structure. Particularly, due to the interaction with procyanidin, the PEF-treated complex exhibited better water-holding capacity, higher apparent viscosity, shear thinning performance, and more stable flow behavior than single inulin. The PEF-treated complex gel also exhibited relatively high hardness, chewiness, and viscosity. Therefore, these results could provide theoretical foundations for PEF treatment to promote the interaction between polyphenols and polysaccharides, which also further broaden the application of inulin-polyphenol complexes in the food industry as water retention agents, texture modifiers, gelling agents, and stabilizers.

CRediT authorship contribution statement

Yuqi Huang: Investigation, Data curation, Writing – original draft. **Ziqi Guo:** Investigation. **Zhe Chen:** Visualization, Software. **Dan Lei:** Investigation. **Shuyi Li:** Conceptualization, Methodology, Formal analysis, Writing – review & editing. **Zhenzhou Zhu:** Resources, Project administration, Funding acquisition. **Francisco J. Barba:** Conceptualization, Supervision. **Shuiyuan Cheng:** Supervision.

Declaration of Competing Interest

The authors declare that they have no known competing financial interests or personal relationships that could have appeared to influence the work reported in this paper.

Data availability

The data that has been used is confidential.

Acknowledgements

This work was supported by Outstanding young and middle-aged science and technology innovation team in Hubei Province (T2020012), Key Research and Development Program of Hubei Province (2020BBA043), Hubei Province International Cooperation Project (2022EHB028), and Key Innovation Team in Enshi Tujia and Miao Autonomous Prefecture, 2020.

Appendix A. Supplementary data

Supplementary data to this article can be found online at https://doi.org/10.1016/j.fochx.2023.100635.

References:

Ding, M., Liu, Y., Ye, Y., Zhang, J., & Wang, J. (2021). Polysaccharides from the lignified okra: Physicochemical properties and rheological properties. *Bioactive Carbohydrates and Dietary Fibre, 26*, Article 100274. https://doi.org/10.1016/j.bcdf.2021.100274

Dong, M., Tian, H., Xu, Y., Han, M., & Xu, X. (2021). Effects of pulsed electric fields on the conformation and gelation properties of myofibrillar proteins isolated from pale, soft, exudative (PSE)-like chicken breast meat: A molecular dynamics study. *Food Chemistry, 342*, Article 128306. https://doi.org/10.1016/j.foodchem.2020.128306

Ganie, S. A., Ali, A., Mir, T. A., & Mazumdar, N. (2019). Preparation, characterization and release studies of folic acid from inulin conjugates. *International Journal of Biological Macromolecules*. https://doi.org/10.1016/j.ijbiomac.2019.10.244

Gao, R., Liu, H., Peng, Z., Wu, Z., Wang, Y., & Zhao, G. (2012). Adsorption of (−)-epigallocatechin-3-gallate (EGCG) onto oat β-glucan. *Food Chemistry, 132*(4), 1936–1943. https://doi.org/10.1016/j.foodchem.2011.12.029

Giteru, S. G., Ali, A., & Oey, I. (2021). Understanding the relationship between rheological characteristics of pulsed electric fields treated chitosan-zein-poly(vinyl alcohol)-polyethylene glycol composite dispersions and the structure-function of their resulting thin-films. *Food Hydrocolloids, 113*, Article 106452. https://doi.org/10.1016/j.foodhyd.2020.106452

Giteru, S. G., Oey, I., & Ali, M. A. (2018). Feasibility of using pulsed electric fields to modify biomacromolecules: A review. *Trends in Food Science & Technology, 72*, 91–113. https://doi.org/10.1016/j.tifs.2017.12.009

Guo, Q., Ma, Q., Xue, Z., Gao, X., & Chen, H. (2018). Studies on the binding characteristics of three polysaccharides with different molecular weight and flavonoids from corn silk (Maydis stigma). *Carbohydrate Polymers, 198*, 581–588. https://doi.org/10.1016/j.carbpol.2018.06.120

Guo, Z., Huang, Y., Huang, J., Li, S., Zhu, Z., Deng, Q., & Cheng, S. (2022). Formation of protein-anthocyanin complex induced by grape skin extracts interacting with wheat gliadins: Multi-spectroscopy and molecular docking analysis. *Food Chemistry, 385*, Article 132702. https://doi.org/10.1016/j.foodchem.2022.132702

Jakobek, L., & Matić, P. (2019). Non-covalent dietary fiber-polyphenol interactions and their influence on polyphenol bioaccessibility. *Trends in Food Science & Technology, 83*, 235–247. https://doi.org/10.1016/j.tifs.2018.11.024

Jin, W., Wang, Z., Peng, D., Shen, W., Zhu, Z., Cheng, S., … Huang, Q. (2020). Effect of pulsed electric field on assembly structure of α-amylase and pectin electrostatic complexes. *Food Hydrocolloids, 101*, Article 105547. https://doi.org/10.1016/j.foodhyd.2019.105547

Jing, Y., Huang, J., & Yu, X. (2019). Maintenance of the antioxidant capacity of fresh-cut pineapple by procyanidin-grafted chitosan. *Postharvest Biology and Technology, 154*, 79–86. https://doi.org/10.1016/j.postharvbio.2019.04.022

Lei, D., Li, J., Zhang, C., Li, S., Zhu, Z., Wang, F., … Grimi, N. (2022). Complexation of soybean protein isolate with β-glucan and myricetin: Different affinity on 7S and 11S globulin by QCM-D and molecular simulation analysis. *Food Chemistry: X, 15*, Article 100426. https://doi.org/10.1016/j.fochx.2022.100426

Li, S., Lei, D., Zhu, Z., Cai, J., Manzoli, M., Jicsinszky, L., … Cravotto, G. (2021). Complexation of maltodextrin-based inulin and green tea polyphenols via different ultrasonic pretreatment. *Ultrasonics Sonochemistry, 74*, Article 105568. https://doi.org/10.1016/j.ultsonch.2021.105568

Li, S., Li, J., Zhu, Z., Cheng, S., He, J., & Lamikanra, O. (2020). Soluble dietary fiber and polyphenol complex in lotus root: Preparation, interaction and identification. *Food Chemistry, 314*, Article 126219. https://doi.org/10.1016/j.foodchem.2020.126219

Li, S., Xiao, J., Chen, L., Hu, C., Chen, P., Xie, B., & Sun, Z. (2012). Identification of A-series oligomeric procyanidins from pericarp of Litchi chinensis by FT-ICR-MS and LC-MS. *Food Chemistry, 135*(1), 31–38. https://doi.org/10.1016/j.foodchem.2012.04.039

Li, S., Xu, H., Sui, Y., Mei, X., Shi, J., Cai, S., … Zhu, Z. J. F. (2022). Comparing the LC-MS Phenolic Acids Profiles of Seven Different Varieties of Brown Rice (Oryza sativa L.). *Foods, 11*(11), 1552. https://doi.org/10.3390/foods11111552

Li, S., Zhang, R., Lei, D., Huang, Y., Cheng, S., Zhu, Z., … Cravotto, G. (2021). Impact of ultrasound, microwaves and high-pressure processing on food components and their interactions. *Trends in Food Science & Technology, 109*, 1–15. https://doi.org/10.1016/j.tifs.2021.01.017

Li, X., Wu, Q., Sui, Y., Li, S., Xie, B., & Sun, Z. (2018). Dietary supplementation of A-type procyanidins from litchi pericarp improves glucose homeostasis by modulating mTOR signaling and oxidative stress in diabetic ICR mice. *Journal of Functional Foods, 44*, 155–165. https://doi.org/10.1016/j.jff.2017.12.024

Lin, L., Shen, M., Liu, S., Tang, W., Wang, Z., Xie, M., & Xie, J. (2018). An acidic heteropolysaccharide from Mesona chinensis: Rheological properties, gelling behavior and texture characteristics. *International Journal of Biological Macromolecules, 107*, 1591–1598. https://doi.org/10.1016/j.ijbiomac.2017.10.029

Liu, D., Lopez Sanchez, P., Martinez Sanz, M., Gilbert, E. P., & Gidley, M. J. (2019). Adsorption isotherm studies on the interaction between polyphenols and apple cell walls: Effects of variety, heating and drying. *Food Chemistry, 282*, 58–66. https://doi.org/10.1016/j.foodchem.2018.12.098

Liu, J., Lu, J., Kan, J., Wen, X., & Jin, C. (2014). Synthesis, characterization and in vitro anti-diabetic activity of catechin grafted inulin. *International Journal of Biological Macromolecules, 64*, 76–83. https://doi.org/10.1016/j.ijbiomac.2013.11.028

Liu, X., Le Bourvellec, C., & Renard, C. M. (2020). Interactions between cell wall polysaccharides and polyphenols: Effect of molecular internal structure. *Comprehensive Reviews In Food Science And Food Safety, 19*(6), 3574–3617. https://doi.org/10.1111/1541-4337.12632

Liu, X., Renard, C. M. G. C., Rolland-Sabaté, A., & Le Bourvellec, C. (2021). Exploring interactions between pectins and procyanidins: Structure-function relationships. *Food Hydrocolloids, 113*, Article 106498. https://doi.org/10.1016/j.foodhyd.2020.106498

Liu, Y., Zhang, Y., Zeng, X., El-Mashad, H., Pan, Z., & Wang, Q. (2014). Effect of pulsed electric field on microstructure of some amino acid group of soy protein isolates. *International journal of food engineering, 10*(1), 113–120. https://doi.org/10.1515/ijfe-2013-0033

López-Gámez, G., Elez-Martínez, P., Martín-Belloso, O., & Soliva-Fortuny, R. (2021). Pulsed electric field treatment strategies to increase bioaccessibility of phenolic and carotenoid compounds in oil-added carrot purees. *Food Chemistry, 364*, Article 130377. https://doi.org/10.1016/j.foodchem.2021.130377

Luft, L., Confortin, T. C., Todero, I., Chaves Neto, Tres, M. V., … Mazutti, M. A. (2021). Extraction and characterization of polysaccharide-enriched fractions from Phoma dimorpha mycelial biomass. *Bioprocess and Biosystems Engineering, 44*(4), 769–783. https://doi.org/10.1007/s00449-020-02486-3

Maniglia, B. C., Pataro, G., Ferrari, G., Augusto, P. E. D., Le-Bail, P., & Le-Bail, A. (2021). Pulsed electric fields (PEF) treatment to enhance starch 3D printing application: Effect on structure, properties, and functionality of wheat and cassava starches. *Innovative Food Science & Emerging Technologies, 68*, Article 102602. https://doi.org/10.1016/j.ifset.2021.102602

Manjón, E., Li, S., Dueñas, M., García-Estévez, I., & Escribano-Bailón, M. T. (2023). Effect of the addition of soluble polysaccharides from red and white grape skins on the polyphenolic composition and sensory properties of Tempranillo red wines. *Food Chemistry, 400*, Article 134110. https://doi.org/10.1016/j.foodchem.2022.134110

Mensink, M. A., Frijlink, H. W., van der Voort Maarschalk, K., & Hinrichs, W. L. J. (2015). Inulin, a flexible oligosaccharide I: Review of its physicochemical characteristics. *Carbohydrate Polymers, 130*, 405–419. https://doi.org/10.1016/j.carbpol.2015.05.026

Niu, D., Zeng, X.-A., Ren, E.-F., Xu, F.-Y., Li, J., Wang, M.-S., & Wang, R. (2020). Review of the application of pulsed electric fields (PEF) technology for food processing in China. *Food Research International, 137*, Article 109715. https://doi.org/10.1016/j.foodres.2020.109715

Pan, H., Xu, X., Qian, Z., Cheng, H., Shen, X., Chen, S., & Ye, X. (2021). Xanthan gum-assisted fabrication of stable emulsion-based oleogel structured with gelatin and proanthocyanidins. *Food Hydrocolloids, 115*, Article 106596. https://doi.org/10.1016/j.foodhyd.2021.106596

Peng, B., Li, Z., Xiong, Q., Wu, C., Huang, J., Zhou, R., & Jin, Y. (2022). Casein-dextran complexes subjected to microfiltration: Colloidal properties and their corresponding processing behaviors. *Journal of Food Engineering, 320*, Article 110913. https://doi.org/10.1016/j.jfoodeng.2021.110913

Shao, P., Qin, M., Han, L., & Sun, P. (2014). Rheology and characteristics of sulfated polysaccharides from chlorophytan seaweeds Ulva fasciata. *Carbohydrate Polymers, 113*, 365–372. https://doi.org/10.1016/j.carbpol.2014.07.008

Spizzirri, U., Altimari, I., Puoci, F., Parisi, O., Iemma, F., & Picci, N. (2011). Innovative antioxidant thermo-responsive hydrogels by radical grafting of catechin on inulin chain. *Carbohydrate Polymers, 84*(1), 517–523. https://doi.org/10.1016/j.carbpol.2010.12.015

Staroszczyk, H., Kusznierewicz, B., Malinowska-Pańczyk, E., Sinkiewicz, I., Gottfried, K., & Kołodziejska, I. (2020). Fish gelatin films containing aqueous extracts from phenolic-rich fruit pomace. *LWT- Food Science and Technology, 117*, Article 108613. https://doi.org/10.1016/j.lwt.2019.108613

Sui, Y., Zheng, Y., Li, X., Li, S., Xie, B., & Sun, Z. (2016). Characterization and preparation of oligomeric procyanidins from Litchi chinensis pericarp. *Fitoterapia, 112*, 168–174. https://doi.org/10.1016/j.fitote.2016.06.001

Taha, A., Casanova, F., Šimonis, P., Jonikaitė-Švėgždienė, J., Jurkūnas, M., Gomaa, M. A. E., & Stirkė, A. (2022). Pulsed electric field-assisted glycation of bovine serum albumin/starch conjugates improved their emulsifying properties. *Innovative Food Science & Emerging Technologies, 82*, Article 103190. https://doi.org/10.1016/j.ifset.2022.103190

Tarone, A. G., Silva, E. K., Betim Cazarin, C. B., & Marostica Junior, M. R. (2021). Inulin/fructooligosaccharides/pectin-based structured systems: Promising encapsulating matrices of polyphenols recovered from jabuticaba peel. *Food Hydrocolloids, 111*, Article 106387. https://doi.org/10.1016/j.foodhyd.2020.106387

Tripodo, G., & Mandracchia, D. (2019). Inulin as a multifaceted (active) substance and its chemical functionalization: From plant extraction to applications in pharmacy, cosmetics and food. *European Journal of Pharmaceutics Biopharmaceutics*. https://doi.org/10.1016/j.ejpb.2019.05.011

Wang, J., Xie, B., & Sun, Z. (2021). The improvement of carboxymethyl β-glucan on the antibacterial activity and intestinal flora regulation ability of lotus seedpod procyanidins. *LWT, 137*, Article 110441. https://doi.org/10.1016/j.lwt.2020.110441

Wang, L., Zhang, B., Xiao, J., Huang, Q., Li, C., & Fu, X. (2018). Physicochemical, functional, and biological properties of water-soluble polysaccharides from Rosa roxburghii Tratt fruit. *Food Chemistry, 249*, 127–135. https://doi.org/10.1016/j.foodchem.2018.01.011

Wu, Z., Ming, J., Gao, R., Wang, Y., Liang, Q., Yu, H., & Zhao, G. (2011). Characterization and antioxidant activity of the complex of tea polyphenols and oat β-glucan. *Journal of Agricultural Food Chemistry, 59*(19), 10737–10746. https://doi.org/10.1021/jf202722w

Yang, H., Tuo, X., Wang, L., Tundis, R., Portillo, M. P., Simal-Gandara, J., … Deng, J. (2021). Bioactive procyanidins from dietary sources: The relationship between bioactivity and polymerization degree. *Trends in Food Science & Technology, 111*, 114–127. https://doi.org/10.1016/j.tifs.2021.02.063

Yi, Y., Tang, H.-S., Sun, Y., Xu, W., Min, T., & Wang, H.-X. (2022). Comprehensive characterization of lotus root polysaccharide-phenol complexes. *Food Chemistry, 366*, Article 130693. https://doi.org/10.1016/j.foodchem.2021.130693

Zhang, L., Zhang, Z., Chen, Y., Ma, X., & Xia, M. (2021). Chitosan and procyanidin composite films with high antioxidant activity and pH responsivity for cheese packaging. *Food Chemistry, 338*, Article 128013. https://doi.org/10.1016/j.foodchem.2020.128013

Zhang, Z., Han, Z., Zeng, X., & Wang, M. (2017). The preparation of Fe-glycine complexes by a novel method (pulsed electric fields). *Food Chemistry, 219*, 468–476. https://doi.org/10.1016/j.foodchem.2016.09.129

Zhu, Z., Huang, Y., Luo, X., Wu, Q., He, J., Li, S., & Barba, F. J. (2019). Modulation of lipid metabolism and colonic microbial diversity of high-fat-diet C57BL/6 mice by inulin with different chain lengths. *Food Research International, 123*, 355–363. https://doi.org/10.1016/j.foodres.2019.05.003

Zhu, Z., Luo, X., Yin, F., Li, S., & He, J. (2018). Clarification of Jerusalem Artichoke Extract Using Ultra-filtration: Effect of Membrane Pore Size and Operation Conditions. *Food and Bioprocess Technology, 11*(4), 864–873. https://doi.org/10.1007/s11947-018-2054-0